Effect of Inclusion of 1-Butyl-3-Methylimidazolium Trifluoromethanesulfonate on CO_2 and N_2Permeabilities for PVDF and PVDF-HFP Membranes

Takashi Makino[1,*], Mitsuhiro Kanakubo[1] and Tadashi Uragami[2,*]

[1]*Research Institute for Chemical Process Technology, National Institute of Advanced Industrial Science and Technology, 4-2-1 Nigatake, Miyagino-ku, Sendai, 983-8551, Japan*

[2]*Department of Chemistry and Materials Engineering, Kansai University, 3-3-35 Yamate-cho, Suita, Osaka 564-8680, Japan*

Abstract: The CO_2 and N_2 permeabilities for polymer inclusion membranes, consisting of 1-butyl-3-methylimidazolium trifluoromethanesulfonate ([bmim][TfO]) in poly (vinylidenedifluoride) (PVDF) and poly (vinilidenedifluoride-co-hexafluoropropylene) (PVDF-HFP), at the temperatures from 298.2 K to 348.2 K, have been evaluated. The PVDF and PVDF-HFP membranes, containing 75 wt% of [bmim][TfO], had the CO_2 permeabilities of 585 and 976 barrers, respectively, and the CO_2 selectivities of 15 at 348.2 K. These values were higher than those of the supported ionic liquid membrane of [bmim][TfO] (428 barrers and 12). Furthermore, the Differential scanning calorimetry and Raman spectroscopy were performed to analyze the micro-structures of membranes. These analyses indicate that the polymer matrix was plasticized and the polymorphs changed from the non-polar α-phase to the polar β-phase by the addition of [bmim][TfO]. According to the solution-diffusion transport mechanism, it is concluded that the inclusion membranes with the sufficiently plasticized, *i.e.* phase-changed, PVDF and PVDF-HFP membranes absorbed the larger amount of gas species than the neat [bmim][TfO], and PVDF-HFP is more effective than PVDF for the enhancement in gas absorption.

Keywords: PVDF, PVDF-HFP, Ionic liquid, Membrane, CO_2 separation.

1. INTRODUCTION

Ionic liquids (ILs) are salts with a melting point at or below ambient temperatures. They are generally non-volatile, non-flammable, and thermally and chemically stable. In addition, ILs can dissolve various chemicals by chemical modifications on cation and anion. Therefore, ILs has attracted much attention as separation media for a variety of chemical processes. One of the promising separation technologies using ILs is CO_2 capture, because ILs do not dissolve in the gas phase even at high pressures as demonstrated in the literature [1]. A number of studies have been performed for the absorption, adsorption, and membrane separation using ILs. The membrane separation can commonly reduce amount of operation energy and footprint of equipment than other separation technologies.

Supported ionic liquid membranes (SILMs), composed of porous organic or inorganic materials filled with ILs, have been researched. SILMs are stable for a much longer time than the supported liquid membrane using organic solvents because of non-volatility of ILs. Furthermore, it is pointed out that some of SILMs show the higher CO_2 permeability and selectivity than the conventional polymer membranes [2-5]. However, SILMs cannot work under pressurized conditions because of easily dropout of ILs filled in porous materials. The polymer inclusion membrane is one of the approaches to overcome this serious disadvantage. The earlier studies have summarized that the composite membrane with a smaller polymer content has the higher CO_2 permselectivity [6-12]. Some research groups reported the self-standing inclusion membranes with polymer contents less than 15wt% [7, 12], however, the matrix of these laboratory-synthesized polymers has the function to load the ILs in their network. In other words, the polymer does not contribute to the CO_2 selective permeation, and the maximum performance of inclusion membrane is determined by only the property of IL.

The CO_2 and N_2 permeation in the poly (vinylidenedifluoride) (PVDF) and poly (vinyldenedifluoride-*co*-hexafluoropropylene) (PVDF-HFP) inclusion membranes has been studied in the present work. PVDF and PVDF-HFP are conventional and inexpensive fluorinated polymers, and they have been widely used to prepare composites, in particular, for electrolytes [13-19]. The fluorine atom is Lewis basic in nature, and favorably interacts with the Lewis acidic carbon atom on CO_2. This means that the fluorinated polymers can absorb the larger amount of CO_2 than the non-fluorinated polymers. In general, the ideal selectivity, *S,* between two gas components (*i*, *j*)

*Address correspondence to this author at the Research Institute for Chemical Process Technology, National Institute of Advanced Industrial Science and Technology, 4-2-1 Nigatake, Miyagino-ku, Sendai, 983-8551, Japan;
Tel: +81-22-237-5257; Fax: +81-22-232-7002;
E-mail: makino.t@aist.go.jp, v701489@kansai-u.ac.jp

E-ISSN: 2410-1869/15

for polymeric membranes is expressed as the solution-diffusion transport mechanism: $S = P_i/P_j = (c_i/c_j)(D_i/D_j)$, where P, c, and D stand for the permeability, concentration, and diffusion coefficient of gas species, respectively. If PVDF and PVDF-HFP enhance the CO_2 solubility in the composite, the CO_2 selectivity is improved compared to the SILM, because both CO_2 and N_2 have the similar diffusion coefficients and the ratio hardly depends on temperature [20]. However, these polymers are semi-crystalline, and thus, the pure PVDF and PVDF-HFP membranes are not appropriate for rapid gas permeation due to the limited diffusion of gas component. Actually, Hong *et al*. demonstrated the higher CO_2 selectivity improved by including PVDF-HFP with 1-butyl-3-methylimidazolium tetrafluoroborate ([bmim][BF_4])[21].

In the present study, the CO_2 and N_2 permeabilities using PVDF and PVDF-HFP inclusion membranes, containing 25, 50, and 75 wt% of 1-butyl-3-methylimidazolium trifluoromethanesulfonate ([bmim][TfO]) and at different temperatures, have been studied. In a previous work, it has been already reported that $[TfO]^-$ is one of the effective anions to obtain the high CO_2 selectivity [9]. The chemical structures of the present polymers and IL are shown in Figure **1**. These membranes were analyzed using Differential scanning calorimetry (DSC), Thermal gravimetry (TG), and Raman spectroscopy to investigate the micro-structures of membranes. Finally, the effects of PVDF and PVDF-HFP on the CO_2 permselectivity have been discussed.

2. EXPERIMENTAL

2.1. Materials and Membrane Preparation

PVDF and PVDF-HFP (12 wt% (4.9 mol%) HFP) were obtained from Kureha Co. [bmim][TfO] (99 %) was purchased from Kanto Kagaku Co. *N,N*-dimethylformamide (DMF, 99.5 %) was supplied by Wako Pure Chemical Industries Ltd. CO_2 (>99.990 %) and N_2 (>99.99995 %) were obtained from Showa Denko Gas Products Co., Ltd. and Koatsu Gas Kogyo Co., Ltd., respectively. All chemicals were used without further purification.

A desired weight of PVDF or PVDF-HFP was dissolved in DMF at room temperature under dry N_2 atmosphere. After the complete dissolution, [bmim][TfO] was added under the same atmosphere and further stirred to obtain a homogeneous solution. [bmim][TfO] was dried under vacuum at 323 K for 30 h to remove the residual water just before the preparation. Then, the solution was poured into a stainless steel petridish and DMF was evaporated slowly at 60 °C for ~12 h. After that, the membrane was evacuated at 80 °C for more than ~24 h to remove the residual solvent. Finally, a clear self-standing membrane was obtained. Hereafter, the membranes are named like PVDF-25, which means the PVDF inclusion membrane with 25 wt% [bmim][TfO].

A SILM of [bmim][TfO] was also prepared for comparison. A hydrophilic PTFE membrane (Merck Millipore, JVWP02500) was dipped into [bmim][TfO] under vacuum at room temperature for 24 h. The PTFE filter has a pore size of 0.1 μm, porosity of 80 %, and thickness of 30 μm. The excess IL on the filter surface was wiped up just before the measurement.

2.2. Thermal and Spectroscopic Analyses of Membranes

Thermal analyses were performed for the PVDF and PVDF-HFP membranes using a differential scanning calorimeter (Bruker, DSC3200SA) with increasing temperature from 253 to 423 K, and a thermogravimetry and differential thermal analysis (Bruker, TG-DTA2010SAT) with heating from room temperature to 1073 K. Every measurement was done at a heating rate of 5 $K \cdot min^{-1}$ and under the dry N_2 flow.

The Raman spectra of inclusion membranes were recorded on a NRS-3100 spectrophotometer (JASCO) using a laser diode, of which the excitation wavelength was 531.96 nm. The membrane and polymer powder

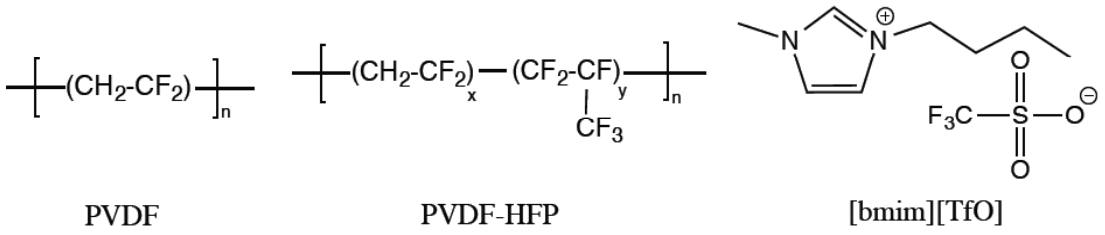

Figure 1: Chemical structures of the present polymers and IL.

were set on a glass plate under atmospheric conditions, and [bmim][TfO] was filled in a vial tube under dry N_2 conditions. The laser was irradiated to the sample from the object lens, and the back scatter was detected with the same lens. The spectral resolution was about 1 cm^{-1} and Raman peaks were calibrated with the Ne emission lines in the air.

2.3. Gas Permeation Measurement

The experimental apparatus and procedure were the same as reported in the previous work [12]. The membrane (diameter 25 mm) was placed on a stainless steel cell with a porous hydrophobic PTFE filter (Advantec Co., T010A025A) as the support. The PTFE filter has a pore size of 0.1 μm, porosity of 68 %, and thickness of 70 μm. The thickness of the membrane was measured with a micrometer. Feed and sweep gases were a CO_2/N_2mixture, of which the CO_2 composition was 50 mol%, and He, respectively. A total pressure of the mixture was 101 kPa (atmospheric pressure). The flow rates of the feed and sweep gases were 50 $cm^3 \cdot min^{-1}$ and 13 $cm^3 \cdot min^{-1}$, respectively, and they were regulated using mass flow controllers (HORIBA STEC Inc., SEC-E40). Neither of the feed and sweep gases contained water in the present study. Temperature was controlled using an oven (ESPEC Co., SH-641). The permeability's of CO_2 and N_2 were evaluated from a flow rate and a composition of the outlet sweep. The flow rate was measured by a film flow meter (HORIBA STEC Inc., SF-1U). The composition was determined using a TCD gas chromatograph (Shimadzu, GC-8A).

3. RESULTS AND DISCUSSION

3.1. Characterization of the Inclusion Membranes

Figure **2** presents the DSC curves of PVDF and PVDF-HFP membranes. PVDF-0 and -25, and PVDF-HFP-0, -25, and -50 did not show any peaks originated from [bmim][TfO] in the present study. On the other hand, an endothermic peak was detected at ~ 280 K for PVDF-50 and -75, and PVDF-HFP-75. These peaks are attributed to the melting of [bmim][TfO], of which the melting temperature is 286 K [22]. An exothermic peak for PVDF-HFP-75 corresponds to the freezing of IL. Other exothermic peaks at high temperatures correspond to the melting of polymer component. These results suggest that the micro phase separation (polymer-rich and IL-rich regions) occurred in the composites with high IL contents. Thus, the fluorinated polymers mixed homogeneously with [bmim] [TfO] at the low IL contents: *i.e*., PVDF and PVDF-HFP are plasticized by the addition of IL. Figure **S1** (ESI) is the TG curves of PVDF and PVDF-HFP membranes and the neat polymers. All the membranes showed two-steps degradation, *i.e*. the decomposition of [bmim][TfO] and the fluorinated polymers. The noticeable weight loss started at ~ 560 K for every membrane.

Figure **3** presents the Raman spectra of the present membranes between 200 and 1200 cm^{-1}. The Raman spectra at higher wave numbers are given for the PVDF and PVDF-HFP membranes in Figures **S2** (ESI) and **S3** (ESI), respectively. Figure **3**-(**a**) shows the Raman spectra of the PVDF membranes. The Raman peaks at 311, 347, 572, 598, 622, 755, 1022, and 1033 cm^{-1} were derived from [bmim][TfO] and detected in the neat IL and the PVDF inclusion membranes. Similarly,

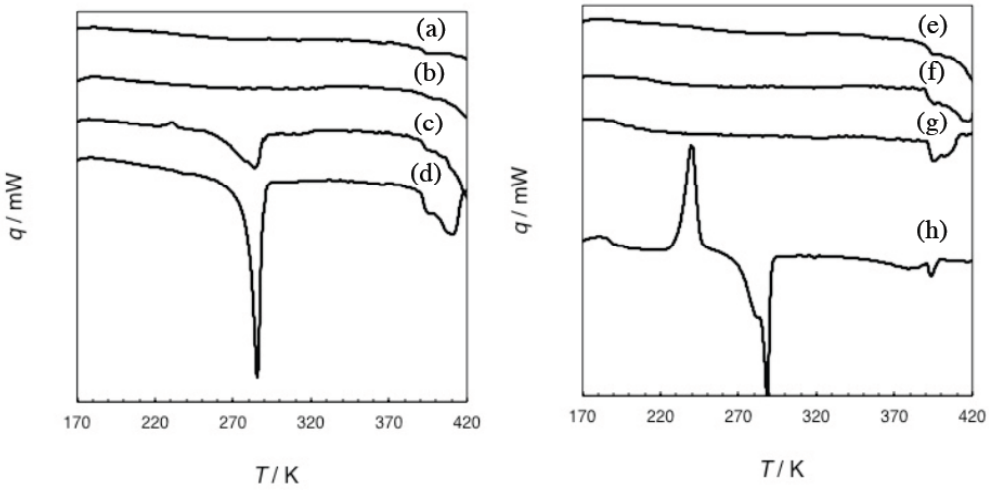

Figure 2: DSC curves for the fluorinated polymer + IL inclusion membranes. (**a**), PVDF-0; (**b**), PVDF-25; (**c**), PVDF-50; (**d**), PVDF-75; (**e**), PVDF-HFP-0; (**f**), PVDF-HFP-25; (**g**), PVDF-HFP-50; (**h**), PVDF-HFP-75.

other peaks of [bmim][TfO] (1116, 1226, 1339, 1388, 1418, 1447, and 1568 cm^{-1}) were observed in every PVDF membrane at higher wave numbers, as shown in Figure **S2**-(**a**). The Raman peaks, from (2800 to 3100) cm^{-1} in Figure **S2**-(**b**), are attributed to the C-H stretching vibrations. The Raman peaks corresponding to [bmim][TfO] did not change significantly, although a little red shift (313, 347, and 755 cm^{-1}) was observed in PVDF-25. The experimental results indicate that a small portion of IL solvates around the PVDF matrix and most IL molecules in the membranes do not interact with the matrix even at the IL content of 25 wt%. The earlier neutron scattering study reported the existence of "free" IL molecules, which behave like neat IL, in the IL + polymer system [23]. The similar results were obtained from the PVDF-HFP as shown in Figures **3**-(**b**) and **S3**.

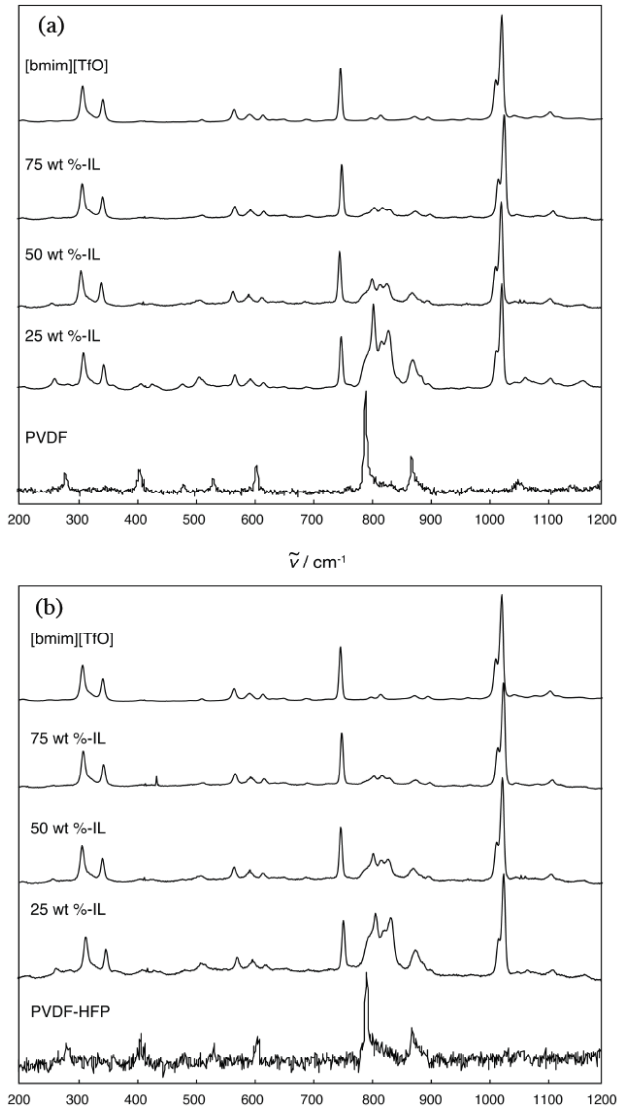

Figure 3: Raman spectra for the fluorinated polymer + IL membranes. (**a**), PVDF + [bmim][TfO]; (**b**), PVDF-HFP + [bmim][TfO].

The Raman peaks at 282, 409, 483, 533, 607, 792, 872, and 1054 $cm^{-1}$are derived from PVDF in Figure **3**-(**a**).The apparent change of Raman spectra between the pure PVDF and the PVDF membranes was observed in the wave number range from (790 to 840) cm^{-1}. The strong peak at 792 cm^{-1} is attributed to the CH_2 rocking and/or C-F stretching vibrations in the α-phase PVDF, which has the *trans-gauche-trans-gauche*(*TGTG'*) conformation [24-27]. This peak was not observed in the PVDF composites and three new peaks at 811, 824, and 837 cm^{-1}appeared instead. According to the literature [25-27], the main C-F stretching bands in *TTTT* (β-phase) and *TTTGTTTG'* (γ-phase) conformations were 840 and 816 cm^{-1}, respectively. In addition, the lower wave number peak (811 cm^{-1}) relatively weakened compared to the higher ones with the increment of IL content. Therefore, the Raman spectra reveal that the polymer conformation changed from *gauche* to *trans* (from non-polar α-phase to polar β-phase), which also supports the plasticization of PVDF. The Raman peaks of PVDF presented in Figures **S2**-(**a**) and - (**b**) showed small red and blue shifts, respectively, by including the IL. The Raman spectra for the PVDF-HFP membranes showed the similar composition dependency to those for the PVDF ones, as shown in Figures **3** and **S3**.

3.2. CO_2 and N_2 permselectivities

Figure **4** shows the permeabilities of CO_2 P_{CO2} and N_2 P_{N2}, and the selectivity of CO_2 S_{CO2} for the PVDF and PVDF-HFP inclusion membranes. P_{CO2} for the present PVDF membranes increased with the increment of temperature and IL content. P_{N2} showed the similar composition dependency to P_{CO2}. P_{N2} for PVDF-75 increased with temperature, whilst those for PVDF-25 and -50 had the minimum values at 313 K and 323 K, respectively. Both P_{CO2} and P_{N2} for PVDF-75 were higher than those for the SILM of [bmim][TfO], though the other PVDF membranes showed the lower permeabilities. The temperature dependencies of S_{CO2} for the present PVDF membranes were convex upward with the maximum values at 323 K (PVDF-50 and -75) and 333 K (PVDF-25). S_{CO2} for PVDF-25, -50, and -75 increased in this order at the temperatures lower than 323 K. On the other hand, at the temperatures higher than 323 K, PVDF-50 and - 75 had the almost same S_{CO2}, which is higher than S_{CO2} of the SILM.

P_{CO2} and P_{N2} for the PVDF-HFP membranes showed the similar temperature and composition dependencies to the PVDF composites. Only P_{N2} for PVDF-HFP-25 showed convex downward and the

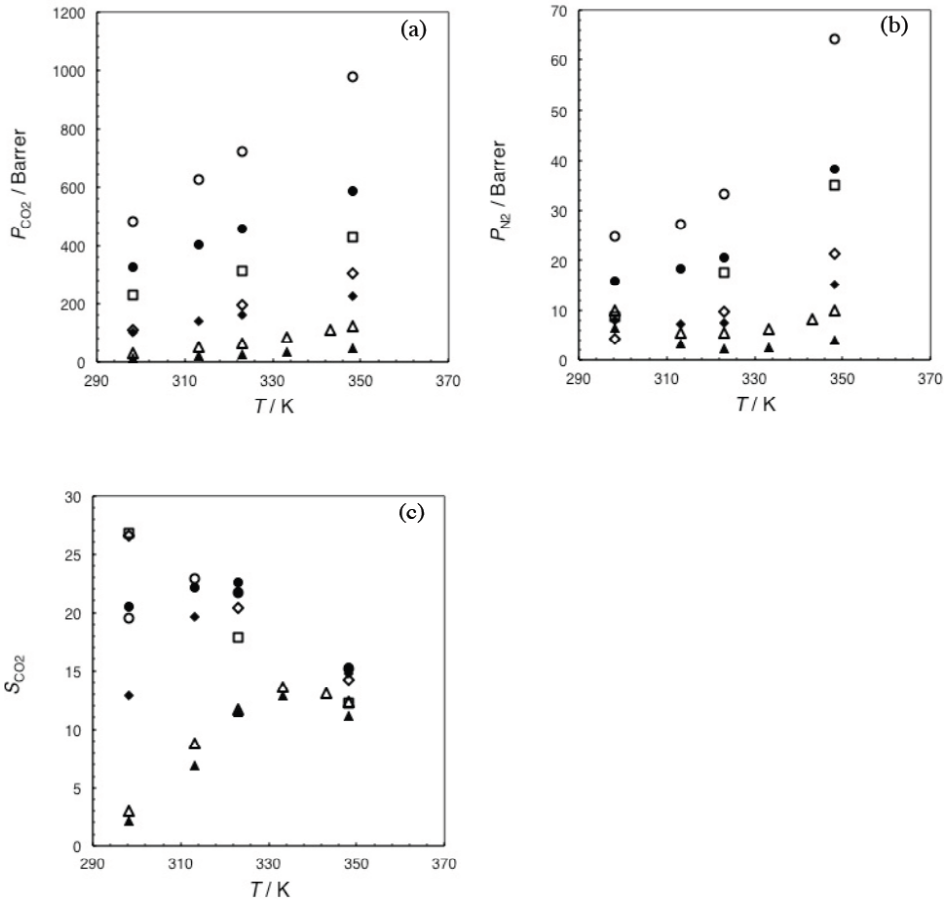

Figure 4: Permeabilities of CO_2 P_{CO2} (**a**) and N_2 P_{N2} (**b**), and selectivity of CO_2 S_{CO2} (**c**) for the inclusion membranes. Closed, PVDF + [bmim][TfO]; open, PVDF-HFP + [bmim][TfO]. Triangle, 25wt%-IL; diamond, 50 wt%-IL; circle, 75 wt%-IL. Open square, SILM of [bmim][TfO].

minimum was observed at 313 K. Both P_{CO2} and P_{N2} for the PVDF-HFP composites were higher than those for the PVDF ones under the present conditions, *e.g*. P_{CO2} for PVDF-HFP-75 at 348 K was ~66 % higher than that for PVDF-75. S_{CO2} for PVDF-HFP-50 decreased with the temperature increment, and those for PVDF-HFP-25 and -75 showed convex upwards, of which the maximums were obtained at 313 K and 333 K. S_{CO2} for the PVDF and PVDF-HFP membranes were almost equal to each other except S_{CO2} for PVDF-50 and PVDF-HFP-50 at 298 and 313 K.

The previous study pointed out that the cross sectional area, where gas molecules contact with the IL, causes the difference in permeabilities between the inclusion membrane and the SILM [12]. Gas molecules can dissolve into the inclusion membrane on the all surface, while the support surface of SILM is not effective for the gas dissolution. The porosity of the present support is 80%, and thus, the "ideal" permeability of SILM is 1.25 times higher than the experimental value. Figure **5** summarizes the ratio of permeability P_i/P_i^{SILM} (i = CO_2 and N_2), P_i^{SILM} stands for the ideal permeability of corresponding gas. When the value is larger than unity, gas molecules permeate through the inclusion membrane more effectively. Figure **5**-(**a**) presents that P_{CO2} for PVDF-25 and -50 were ~6 and ~40 % of that for the SILM and P_{CO2}/P_{SILM} did not depend temperature significantly. P_{CO2}/P_{SILM} for PVDF-75 are higher than unity, and decreased by heating. P_{N2}/P_{SILM} showed the steep decrement at the low temperatures and the gradual decrement at the high temperatures. For the ratio for PVDF-HFP membranes, Figure **5**-(**b**) reveals that the temperature and composition dependencies of P_i/P_{SILM} were similar to those for PVDF membranes, where as the values of P_i/P_i^{SILM} were larger than those for PVDF membranes.

Generally, the addition of polymer increases the viscosity of IL, resulting in the decrement of diffusion of gas species. According to the solution-diffusion transport mechanism, $1 < P_i/P_i^{SILM}$ suggests that the polymer enhances the gas solubility, and then, the composites, PVDF-75 and PVDF-HFP-75, absorbed the larger amount of gas species than the neat [bmim][TfO]. One of the reasons for the improvement of

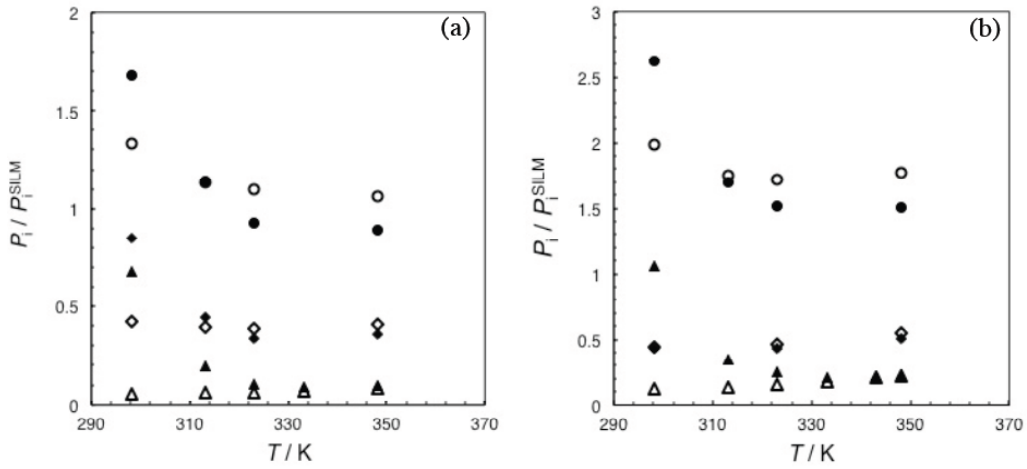

Figure 5: Ratio of permeability P_i/P_{SILM} for the PVDF + [bmim][TfO] (**a**) and PVDF-HFP + [bmim][TfO] (**b**) inclusion membranes. Closed, P_{N2}/P_{SILM}; open, P_{CO2}/P_{SILM}. Triangle, 25wt%-IL; diamond, 50 wt%-IL; circle, 75 wt%-IL.

P_{CO2} might be the high content of fluorine atom in the polymers. On the other hand, the inclusion membranes with 25 and 50 wt% - IL showed smaller P_i/P_i^{SILM}, that is, the fluorinated polymers do not improve the gas solubility significantly when the IL content is not enough. The slower diffusion of gas species due to the rigid matrix is also the reason of smaller permeability. The thermal and spectroscopic analyses indicated that both the fluorinated polymers were plasticized, and the polymorphs changed from the non-polar α-phase to polar β-phase with increasing the IL content. Commonly, the polar material is more CO_2-philic than the non-polar material due to the quadrupole moment of CO_2. Therefore, PVDF and PVDF-HFP, which are sufficiently plasticized (phase-changed) by the IL, can contribute to the improvement of gas solubility. It is well known that the copolymerization of HFP decreases the melting point, *i.e*. crystallinity, of PVDF. Thus, it is suggested that the higher permeability for PVDF-HFP composites is due to the lower crystallinity, that is, the easy plasticization.

4. CONCLUSION

The CO_2 and N_2 permeabilities of the [bmim][TfO]-PVDF and [bmim][TfO]-PVDF-HFP membranes were measured. Both the permeabilities generally become higher with increasing temperature and IL content. The PVDF and PVDF-HFP membranes with 75 wt% of [bmim][TfO] showed the higher CO_2 permeability and selectivity than the “ideal” SILM. The DSC and Raman spectroscopy indicated that the most part of [bmim][TfO] in the membranes behave like the neat IL, in which [bmim][TfO] performs as a plasticizer of PVDF and PVDF-HFP. The polymers were plasticized (phase-changed) enough at the IL content of 75 wt% to improve the gas solubility in inclusion membranes. This conformation change from non-polar α-phase to polar β-phase causes the enhancement of CO_2 solubility in the inclusion membranes, resulting in the higher permeability and selectivity compared to the SILM. The more intense effect for PVDF-HFP is attributed to the lower crystallinity.

ACKNOWLEDGEMENT

T.M. would thank to Prof. Yusuke Hiejima and Mr. Atsuhiro Oguni for the useful discussion and the assistance with the measurement, respectively. This work was partially supported by Iketani Science and Technology Foundation.

SUPPLEMENTAL MATERIALS

The supplemental materials can be downloaded from the journal website along with the article.

REFERENCES

[1] Lynnette LA, Blanchard A, Hancu D, Beckman EJ, Brennecke JF. Nature 1999; 399: 28-9.

[2] Scovazzo P. J Membr Sci 2009; 343: 199-211. http://dx.doi.org/10.1016/j.memsci.2009.07.028

[3] Bara JE, Carlisle TK, Gabriel CJ, Camper D, Finotello A, Gin DL, *et al.* Ind Eng Chem Res 2009; 48: 2739-51. http://dx.doi.org/10.1021/ie8016237

[4] Mahurin SM, Lee JS, Baker GA, Luo H, Dai S. J Membr Sci 2010; 353: 177-183. http://dx.doi.org/10.1016/j.memsci.2010.02.045

[5] Close JJ, Farmer K, Moganty SS, Baltus RE. J Membr Sci 2012; 401-402: 201-10. http://dx.doi.org/10.1016/j.memsci.2011.11.037

[6] Hudiono YC, Carlisle TK, Bara JE, Zhang Y, Gin DL, Noble RD. J Membr Sci 2010; 350: 117-23. http://dx.doi.org/10.1016/j.memsci.2009.12.018

[7] Gu Y, Lodge TP. Macromolecules 2011; 44: 1732-36. http://dx.doi.org/10.1021/ma2001838

[8] Jansen JC, Friess K, Clarizia G, Schauer J, Izák P. Macromolecules 2011; 44: 39-45. http://dx.doi.org/10.1021/ma102438k

[9] Li P, Pramoda KP, Chung TS. Ind Eng Chem Res 2011; 50: 9344-53. http://dx.doi.org/10.1021/ie2005884

[10] Tomé LC, Mecerreyes D, Freire CSR, Rebelo LPN, Marrucho IM. J Membr Sci 2013; 428: 260-6. http://dx.doi.org/10.1016/j.memsci.2012.10.044

[11] Kasahara S, Kamio E, Yoshizumi A, Matsuyama H. Chem. Commun 2014; 50, 2996-99. http://dx.doi.org/10.1039/C3CC48231F

[12] Fujii K, Makino T, Hashimoto K, Sakai T, Kanakubo M, Shibayama M, Chem Lett 2015; 44: 17-9. http://dx.doi.org/10.1246/cl.140795

[13] Kim KS, Park SY, Yeon SH, Lee H. Electrochim Acta 2005; 50: 5673-8. http://dx.doi.org/10.1016/j.electacta.2005.03.044

[14] Sutto TE, J Electrochem Soc 2007; 154: P101-7. http://dx.doi.org/10.1149/1.2767414

[15] Lalia BS, Yamada K, Hundal MS, Park JS, Park GG, Lee QY, Kim CS, Sekhon SS. Appl Phys A 2009; 96: 661-70. http://dx.doi.org/10.1007/s00339-009-5129-y

[16] Pandey GP, Hashmi SA. J Mater Chem A 2013; 1: 3372-8. http://dx.doi.org/10.1039/c2ta01347a

[17] Chaurasia SSK, Singh RK, Chandra S. J Phys Chem B 2013; 117: 897-906. http://dx.doi.org/10.1021/jp307694q

[18] Singh SVK, Singh RK. J Mater Chem C 2015; 3: 7305-18. http://dx.doi.org/10.1039/C5TC00940E

[19] Yuan C, Zhu X, Su L, Yang D, Wang Y, Yang K, *et al.* Colloid Polym Sci 2015; 293: 1945-52. http://dx.doi.org/10.1007/s00396-015-3590-z

[20] Thomas MK, Heller A, Rausch MH, Wasserscheid P, Economou IG, Fröba AP. J Phys Chem B 2015; 119: 8583-92. http://dx.doi.org/10.1021/acs.jpcb.5b02659

[21] Hong SU, Park D, Ko Y, Baek I. Chem Commun 2009; 7227-9. http://dx.doi.org/10.1039/b913746g

[22] Fredlake CP, Crosthwaite JM, Hert DG, Aki SNVK, Brennecke JF. J Chem Eng Data 2004; 49: 954-64. http://dx.doi.org/10.1021/je034261a

[23] Kofu M, Someya T, Tatsumi S, Ueno K, Ueki T, Watanabe M, *et al.* Soft Matter 2012; 8: 7888-97. http://dx.doi.org/10.1039/c2sm25348h

[24] Kobayashi M, Tashiro K, Tadokoro H. Macromolecules 1975; 8: 158-71. http://dx.doi.org/10.1021/ma60044a013

[25] Tashiro K, Kobayashi M, Polymer 1988; 29: 426-36. http://dx.doi.org/10.1016/0032-3861(88)90359-X

[26] Zheng J, He A, Li J, Han CC. Macromol Rapid Commun 2007; 28: 2159-62. http://dx.doi.org/10.1002/marc.200700544

[27] Tao M, Liu F, Ma B, Xue L. Desalination 2013; 316: 137-45. http://dx.doi.org/10.1016/j.desal.2013.02.005

Received on 30-10-2015 Accepted on 12-11-2015 Published on 27-11-2015

http://dx.doi.org/10.15379/2410-1869.2015.02.02